

Diagnosis of Retinitis Pigmentosa from Retinal Images

Giritharan Ravichandran, Poonguzhali Elangovan, and Malaya Kumar Nath

Abstract—Retinitis pigmentosa is a genetic disorder that results in nyctalopia and its progression leads to complete loss of vision. The analysis and the study of retinal images are necessary, so as to help ophthalmologist in early detection of the retinitis pigmentosa. In this paper fundus images and Optical Coherence Tomography images are comprehensively analyzed, so as to obtain the various morphological features that characterize the retinitis pigmentosa. Pigment deposits, important trait of RP is investigated. Degree of darkness and entropy are the features used for analysis of PD. The darkness and entropy of the PD is compared with the different regions of the fundus image which is used to detect the pigments in the retinal image. Also the performance of the proposed algorithm is evaluated by using various performance metrics. The performance metrics are calculated for all 120 images of RIPS dataset. The performance metrics such as sensitivity, sensibility, specificity, accuracy, F-score, equal error rate, conformity coefficient, Jaccard's coefficient, dice coefficient, universal quality index were calculated as 0.72, 0.96, 0.97, 0.62, 0.12, 0.09, 0.59, 0.45 and 0.62, respectively.

Keywords—Retinitis pigmentosa, Pigment deposits, Retinal fundus image, Blood vessel extraction, watershed segmentation

I. INTRODUCTION

THERE are many defects and diseases of eye that need to be addressed so as to ensure its proper functioning. The defects in eye includes diabetic retinopathy, compressive optic neuropathy, glaucomatous optic neuropathy, glaucoma, ocular hypertension, retinitis pigmentosa [1]–[4]. There will be significant changes in physiology of eye due to various diseases and disorders. If we take diabetic retinopathy, we could find exudates which are basically proteins and lipids deposition. Also it is characterized by the hemorrhages. There are different techniques in which image can be acquired. They include fundus image and optical coherence tomography. The fundus image gives the 2D structure of eye. Retinal fundus image is characterized by different regions that include blood vessels, optic disc, fovea, macula, and optic cup as shown in Figure 1. It also contains rods and cones. Rods correspond to dark light vision, and cones correspond to normal light vision. Optical coherence tomography gives the 3D structure of the retina, where the depth of different layers are analyzed [5]. On looking into the image of OCT with reference to the depth it is classified as many layers such as nerve fiber layer, outer plexiform layer, ganglion cell layer, outer nuclear layer,

R. Giritharan is with the Department of Electronics and Communication Engineering, E.G.S. Pillay Engineering College, Nagapattinam, TN, 611001 INDIA (e-mail: giritharan101995@gmail.com).

E. Poonguzhali and Malaya Kumar Nath are with Department of Electronics and Communication Engineering, NIT Puducherry, Karaikal, PY, 609609 INDIA (e-mail: epoonguzhali3@gmail.com, malaya.nath@nitpy.ac.in).

inner plexiform layer, retinal pigment epithelium, outer segment, inner segment, external limiting membrane and interface between IS and OS [1].

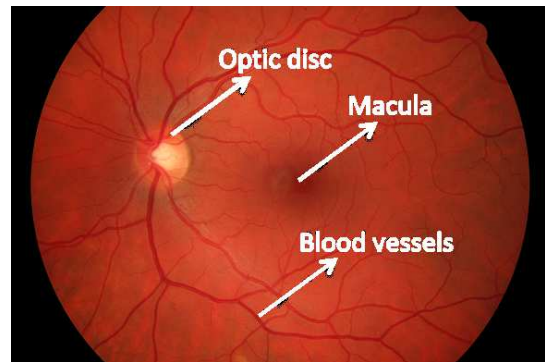


Fig. 1. Normal features of retina

This article gives the comprehensive study of the genetic disorder Retinitis Pigmentosa (RP), focusing on progress and diagnosis of the RP at early stage. The important morphological characteristics of various elements that get changed due to RP, with significance towards the pigment deposits is discussed. The paper is organized as follows: Section 2 describes the characteristics of RP and PD. Proposed method for detection of PD is investigated in Section 3. Section 4 discusses in detail about various results along with the performance metrics and in Section 5, some conclusions are drawn.

II. CHARACTERISTICS OF RP AND PD

A. Retinitis Pigmentosa

RP is the retinal dystrophies or rod cone dystrophy [6]. It is a genetic disorder which results in progressive degradation of the vision. It is initially characterized by night blindness (Nyctalopia), which at later stages lead to vision loss. It also leads to Photopsia and can also lead to loss of side vision called as peripheral vision. RP as said earlier is a genetic disorder that is inherited. It occurs due to the changes in one or more than one of the 50 genes of 50 [6], [7]. These genes are called as photoreceptors, which contain instruction for making proteins required in retina. Due to the significant changes in the genes, it could not make the proteins required and hence limits the functions of the cells. In some cases, it also produces toxic proteins in the cell. Still in other cases

it produces abnormal protein that function in an improper manner. In each case, it leads to significant degradation of the photoreceptors. Conversion of light signals to electrical signals happens due to photoreceptors, which include rods and cones. These electrical signals are sent to other cells and finally to the optic nerve which connects into the visual region of brain, so that the brain can perceive the image.

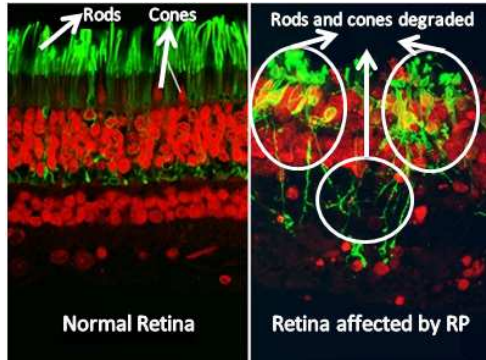


Fig. 2. Normal and RP patients retina

The diagram shown in Figure 2 shows the images of the normal retina and retina of the patients with RP. It is clearly seen that the photoreceptors, the rods and cones are degraded. This degradation is due to the pigment deposits (PD) the cause of which is discussed in the later part of the paper. Due to this degradation, the vision of patients with RP gradually deteriorates. RP is a rare disease, reported roughly 1 in 4000 people worldwide [6], [7]. Every human contains chromosomes of 23 pairs. Out of these 23 pairs, 22 are of body chromosome and 1 is sex chromosome. This sex chromosome pair is contributed by each parent at conception through egg and sperm cells. It is on this basis the sex of the human is defined. The sex chromosomes are X and Y. When a child has X inherited from both parent (i.e) XX pair, the child is said to be female. When one of the parents contributes X and other contribute Y leading to XY pair, results in male child. The pairs other than sex chromosome are called as autosomes. The autosomes are the one which contains non-sex traits. RP occurs in any one of the following three cases.

a) *Autosomal Recessive Inheritance*: Two copies of mutant gene are taken which results in disorder. A person with Recessive Gene Mutation (RGM) is described as a carrier [7]–[9]. When both the parents are carriers the probabilities are described in Table I.

TABLE I
PROBABILITY OF AUTOSOMAL RECESSIVE INHERITANCE

	Probability P(i)
Child with RP disorder	0.25
Child with carrier gene	0.50
Child neither with disorder nor carrier	0.25

b) *Autosomal Dominant Inheritance*: One, disorder causing mutation gene copy is taken thus resulting the disorder. In

parents with gene mutation dominant, the probability that the children have inherited the mutation resulting in disorder is 0.5 [7]–[9].

c) *X-Linked Inheritance*: Mutated gene X of mother is passed to their sons since females do have two X chromosome. The mutation effect on one X is offset by another normal gene [10]. Inheritance from mother with X linked disorder probability is tabulated in Table II.

TABLE II
PROBABILITY OF X-LINKED INHERITANCE

	Probability P(i)
Son with RP disorder	0.25
Daughter with carrier gene	0.50

The initial stages of symptoms occur in childhood, where often the child finds it uncomfortable getting into the dark. As it evolves, it causes degradation of side vision and things appear clumsy causing Photophobia. The symptoms and progression vary between people. Some do have loss of vision by 50's, others do experience loss of vision in early childhood. Almost all the people affected by RP will lose their sight. At later stages, the differentiation of RP from other diseases is quiet difficult. In children, a change in retinal generation is also observed. At early stages, proper investigation of mid-peripheral region of fundus image of retina gives significant information about RP. Diagnosis of RP include measuring the electrical activity of the photoreceptor, to check whether there is any degradation in the rods and cones. The electrical activity of the retina is recorded using the Electroretinogram (ERG) and it will be deteriorated in RP patients. Another method is genetic testing, where the genetic samples of the patients are analysed for the disorders. In imaging perspective there are two methods of analysing.

- 1) Analysis using optical coherence tomography images, where the thickness of the OS and ONL are measured, which signifies that decrease in thickness results due to RP.
- 2) Analysis using retinal fundus image, which requires a good amount of work so as to extract and analyze features such as darkness and entropy of the retinal fundus image.

B. Diagnosis of RP using Fd-OCT

The optical coherence tomography (OCT), especially frequency domain OCT (Fd-OCT) gives the three dimensional perspective of the human retina, and hence gives the various morphological features with respect to the depth. As seen in the Figure 3, from OCT many different layers could be extracted, of which outer segment (OS) and outer nuclear layer (ONL) are our main focus.

Thickness of outer nuclear layer is contributed by the rod and cone nuclei. In the RP affected patients the pigment deposits are predominant in a 500 micrometer diameter from the center, the fovea. Table III shows that the region with 500 micrometer diameters is zone 4 where the rod nuclei are predominant. Hence, the rods nuclei are degraded (i.e) rod cells die due to the pigment deposits. This degradation

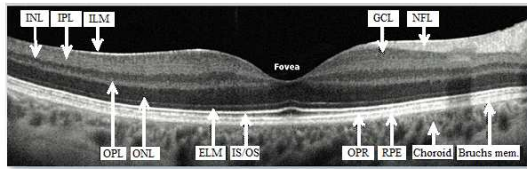


Fig. 3. Optical coherence tomography of retina showing Inner limiting membrane (ILM), inner plexiform layer (IPL), outer nuclear layer (ONL), external limiting membrane (ELM), junction of inner and outer photoreceptor segment (IS/OS), outer plexiform layer (OPL), outer segment PR/RPE complex (OPR), nerve fibre layer (NFL), inner nuclear layer (INL), ganglion cell layer (GCL), retinal pigment epithelium and Bruch's membrane.

could be clearly observed in Figure 2. The degradation of the rods leads to nyctalopia. The deposition is not limited to the zone 4. With its progress, the PD propagates even to Zone 3, where the rods and cones nuclei are concentrated. This leads to degradation in the vision gradually. Only in extreme cases, the PD's are found in Zone 2, which results in complete loss of vision. As a result of comprehensive study it could be concluded that, RP leads to thinning of outer segment (OS) followed by the thinning of outer nuclear layer (ONL) [5].

TABLE III

DIFFERENT ZONES AND THEIR DIAMETER WITH FOVEA AS CENTER (AS OBSERVED FROM THE FD-OCT)

Zone	Diameter in micrometer
Rod-free zone (Zone 1)	<350
Zone in which only cones are present (Zone 2)	100-200
Zone where rods and cones are present in equal densities (Zone 3)	400-500
Zone with predominant rod nuclei (Zone 4)	500

C. Pigment deposits

Pigment deposits occur due to RP is commonly concentrated in the mid periphery region, where the rods nuclei are present. Although the PD occurrence may be attributed to many reasons, the major reason for the PD occurrence is due to the RP. Some of the other reasons include crypto-based retinal detachment surgery and rheumatogenous retinal detachment [11]. The pigments are released from the pigment epithelium. This release can be due to the retinal detachment surgery or the genetic disorder RP [11]. The ocular fluids are responsible for carrying the PD to various part of the eye, thus resulting in its deposition. The flow of pigments is characterized either by subretinal fluid direction or transvitreally. The fundus image of RP patient with PD is shown in Figure 4. The images are taken from the single patient with different angle of view. These are obtained from the RIPS dataset. The PDs are marked with white boundary in the image. It is observed that PD's are deposited throughout the fundus image and are concentrated in the peripheral region of the eye, where the rods and cones are present.

There are various works that have previously discussed about pigment deposits that occur due to the retinal detachment

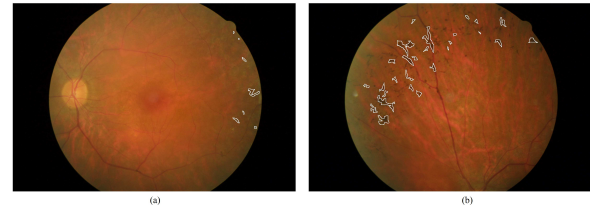


Fig. 4. Fundus Image of RP patient. They are the images of a single patient taken in different angle of view.

surgery. They have discussed about the pigment dispersal, pigment migration, etc., But none of the works are related to the characterization of PD due to the retinitis pigmentosa. The pigment migrations are classified as patchy, striated, spotty and mixed. Based on the location, PD's are classified as subretinal and epiretinal pigment deposits. Basically the PD is characterized different morphological characteristics. They include degree of darkness, edge entropy, mahalanobis distance and mean gray value etc., Here instead of the pixel level processing, the region level processing is done by using the watershed transformation to group the homogeneous regions, which helps in partitioning of the region. Here the watershed transformation segmentation is done to extract the PD from the fundus image of RP Patients.

III. PROPOSED METHOD FOR RP AND PD DETECTION FROM RETINAL IMAGE

A. RP diagnosis

Funduscopy examination is an easier process of image acquisition and analysis. The fundus image is characterized by various components including blood vessels, optic disc, macula and retinal grains. On funduscopy examination; the RP can be characterized by blood vessel attenuation, waxy disc pallor, and pigment deposits. This section gives a comprehensive study on the methods via which these characteristics are used to detect the retinitis pigmentosa.

There are various works done on blood vessel extraction, so as to quantify the blood vessel attenuation due to the retinitis pigmentosa [12]–[14]. Here a direction map is applied over the red channel of the retinal images, thus each pixel is assigned one out of twelve directions [12]. It involves complex operations that include direction mapping, editing, and removal of foreground and background noise. Blood vessels cross section could be approximated by the Gaussian function. Hence a Gaussian shaped filter is designed so as to match the blood vessels which helps in its detection. The problem with this filter is its response to the edges that are not vessels. Thus the output of designed match filter will be the vessels as well edges that are not vessels. To distinguish between the vessels and edges, a pair of filters is used. The matched filter and first order derivative of Gaussian is used [15]. The vessels and the edges are distinguished by the the first order derivative of the Gaussian. The local mean of the image is obtained, normalized and used to calculate the threshold of the image. Binary image

is obtained using the threshold value which gives the extracted blood vessels of RP patients.

Another important trait of the retinitis pigmentosa (RP) is that the optic disc turns pale. This occurs at the later stage of the RP, however this could be analyzed by investigating the optic disc rim color [1], [16] and [2]. The Disc Color Indices (DCI) are calculated that indicates the red intensity in the rim of the optic disc [1]. Here three DCI's are calculated that quantifies the intensity of redness. DCI1, DCI2 and DCI3 are calculated as follows:

$$DCI1 = R/(R + G + B) \quad (1)$$

$$DCI2 = (R - G)/R \quad (2)$$

$$DCI3 = (R - G)/(R + G + B) \quad (3)$$

where,

- R is mean red intensity,
- G is mean green intensity, and
- B is mean blue intensity.

B. PD detection

The complete block diagram of the proposed model is shown in Figure 5.

Pre-processing is needed to be done so as to remove the noise in posterior portion of the image. To reduce the noise the shaded image is obtained. The shaded image is obtained by applying a mean filter of $(7k-1) \times (7k-1)$, where the k is fixed to 10. The noise free shade corrected image I_c is obtained as shown below:

$$I_c = I - I_s \quad (4)$$

where,

- I_c = shade corrected image
- I_s = shaded image
- I = original image

The shade corrected image I_c is enhanced by using contrast limited adaptive histogram equalization (CLAHE). This is done in an independent color space (lab color space). Thus the RGB image is converted into Lab color space and CLAHE is applied and enhanced using luminosity and contrast enhancement. Further the image is converted back to RGB color space to extract the red-channel image. Thus obtained red-channel image is used for further processing since PDs are of more affinity towards black color and hence they are clearly visible in red-channel.

The next process towards PD detection is segmentation. Watershed based segmentation method is used. Basically watershed lines are constructed between the local maxima and minima, and the partitioning is done. This results in the different regions of different morphology. Thus the pixel level processing is now changed to region level processing. The region merging is also done based on the information available at the gray level, thus reducing the number of regions. Here each region is assigned with the median gray level value $G(R)$.

In order to detect the PD, two important features are taken into account which includes the darkness degree and entropy of the edges. Let $Dd(R)$ be the darkness degree of a region R , $Er(R)$ be the entropy of the region R . The darkness of the regions with PD is higher than the darkness in the other regions. The darkness is given by dividing the median gray value as the function of the neighbourhood value of the region R and the median gray value of the given region. Also the entropy $Er(R)$ of the region R is calculated as the entropy of the 10×10 patch in the center of the boundary considered and it is formulated as following:

$$Dd(R) = G(Nr(R))/G(R) \quad (5)$$

$$Er(R) = (Ipi)/nr(R) \quad (6)$$

where,

- $Dd(R)$ - degree of darkness of region R
- $G(R)$ - median gray value of region R
- $Nr(R)$ - median gray value of neighbourhood region of R
- $Er(R)$ - entropy of the region R
- Ipi - entropy of 9×9 patch centered at the boundary of the region R
- $nr(R)$ - median gray value of the neighbourhood region of the patch within the region R

The mahalanobis distance of 97.5 percentile keeps almost all the PD outside the region. The region can be obtained by two ways which include Minimum Covariance Determinant (MCD) estimator [17]. The center of thus identified region is used for the better approximation of the darkness $Md(R)$ and entropy $Mr(R)$ of the normal image other than PD. Thus a region is classified as PD if following condition is satisfied:

$$Dd(R) > Md(R) \quad (7)$$

$$Er(R) > Mr(R) \quad (8)$$

It is possible that some of the low contrast PD are not detected by the above criteria. Hence they are detected by reducing the mahalanobis distance to 90 percentile, only to the regions neighborhood to the regions that are earlier classified as the PD. Almost all the PD are detected, except some of the PD's which are isolated.

IV. RESULTS AND DISCUSSION

The RP patient database is obtained from the RIPS dataset as given by [17]. RIPS dataset consists of 120 images from 4 different subjects. The dataset contains original color retinal image, ground truth model $G1$ and $G2$, and also FoV which contains binary masks as a separate directory. Each directory contains 4 subjects and each subject does have three sessions with time lapse between sessions of one to six months. Each session contains the images of left and right eyes, with each eyes captured in 5 different angle of view. The resolution of the image is $1440 \times 2160 \times 3$.

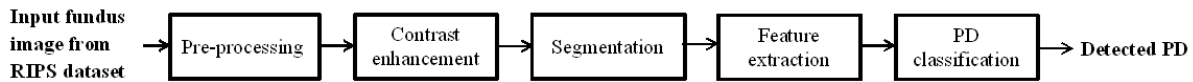


Fig. 5. Block diagram for PD detection

A. RP diagnosis results

The important trait of the RP is the attenuation of the blood vessels. In this Section the blood vessels are extracted so as to observe this. In Figure 6, the blood vessels are extracted for the normal persons and RP patients.

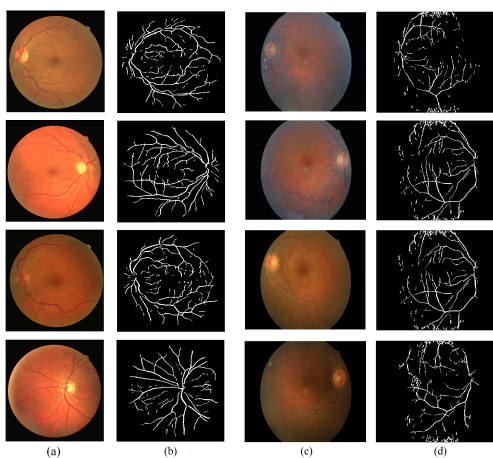


Fig. 6. Blood vessel extraction; (a) Original fundus of normal person, (b) blood vessel extracted image of normal person, (c) Original fundus of RP patient, (d) blood vessel extracted image of RP patient

Another important trait to differentiate the RP patient from normal patient is the color of the optical disk. In order to understand this the color of the optical disk of normal person and RP patient is tabulated in Table IV. Here the normal eyes were taken from the DRIVE Database, and the eyes of patients with RP are obtained from the RIPS dataset. All the eyes were taken from persons with normal visual acuity calculated by logMAR logarithm of minimum resolution angle. It is clearly observed that the DCI1, DCI2 and DCI3 of the RP patient are much less than the DCI's of normal person.

B. PD detection results

The darkness and entropy are important parameters that are helpful in the detection of PD. The darkness degree and the entropy of the various elements of the fundus image are calculated and plotted in the Table V. It is observed that these PD's are comparatively different from other regions with respect to the darkness degree Dd(R) and Entropy Er(R).

TABLE IV
COMPARISON OF DISC COLOR INDICES DCI1, DCI2 AND DCI3 OF THE NORMAL PERSON AND RP PATIENTS

	Normal Person	RP Patient
Number of eyes	120	120
Age in years	55.0 ± 12.6	56.2 ± 14.8
Visual acuity	-0.15 ± 0.06	-0.12 ± 0.04
DCI1	0.56 ± 0.05	0.49 ± 0.08
DCI2	0.43 ± 0.06	0.33 ± 0.04
DCI3	0.24 ± 0.05	0.16 ± 0.07

TABLE V
DARKNESS Dd(R) AND ENTROPY Er(R) OF VARIOUS COMPONENTS OF FUNDUS IMAGE

	Darkness Dd(R)	Entropy Er(R)
Number of eyes	120	120
Age in years	55.0 ± 12.6	56.2 ± 14.8
Visual acuity	-0.15 ± 0.06	-0.12 ± 0.04
Retinal Grains	0.9-1.2	3.5-4.0
Blood Vessels	0.6-1.0	3.0-4.0
Optic Disc	0.5-1.2	2.5-3.0
Pigment Deposits (PD)	1.0-2.2	4.0-5.0
Normal Fundus Regions	0.2-1.2	2.5-5.0

The normal eyes were taken from the DRIVE database, and the eyes of patients with RP are obtained from the RIPS dataset. All the eyes were taken from persons with normal visual acuity calculated by logMAR logarithm of minimum resolution angle. Here the retinal grains and optic disc also fall in the region of the PD in respect to darkness. The optic disc is separated from the PD by means of the field of the region and also with respect to entropy. Also in case of retinal grains, they are segregated with respect to the entropy, and also by the mahalanobis distance. The process of PD detection involves shade correction, contrast enhancement, watershed based segmentation, feature extraction and the PD detection result of 4 patients is shown in Figure 7.

Figure 8 shows the comparison of the detected PD with the Ground Truth models based on which the performance metrics is analysed. The dataset contains the Ground Truth of the PD which are manually annotated by two experts [17]. The segmented image is compared with the Ground Truth and performance measures such as accuracy, sensitivity, specificity, sensibility, equal error rate, f-score, Jaccard's coefficient, conformity coefficient, dice coefficient, mean square error, root mean square error, peak signal-to-noise ratio, mean absolute error, Pearson correlation coefficient, structural content and structural similarity index are calculated [18], [19].

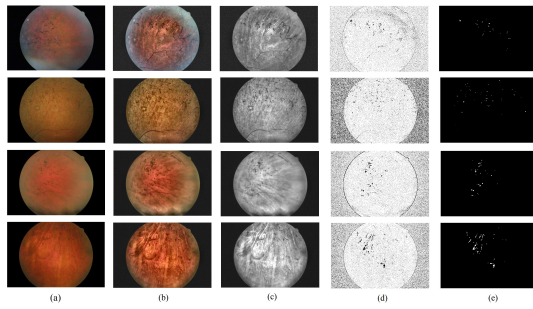


Fig. 7. PD's extracted in the four RP patient from RIPS dataset. [a] original fundus image, [b] shade corrected and contrast enhanced image, [c] extracted red channel image, [d] watershed based segmented image, [e] detected PD.

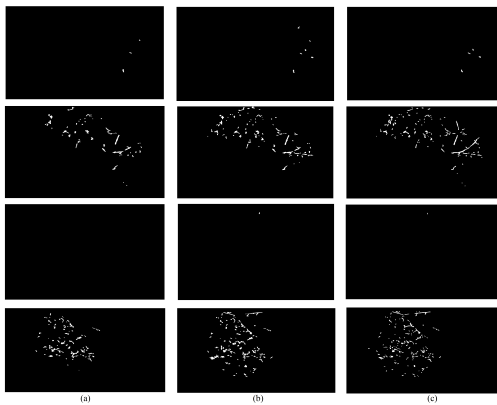


Fig. 8. Comparison of detected PD with the Ground Truth models. (a) Detected PD using proposed model, (b) Ground Truth 1, and (c) Ground Truth 2

The performance metrics are analysed for all the 120 images and are boxplotted. The Figure 9 shows the boxplot of metrics values for 120 images. These values are calculated with respect to the ground truth 1 from the RIPS dataset. Whereas Figure 10 shows the boxplot of metrics values for 120 images with respect to the ground truth 2 from the RIPS dataset. The bottom edge of the box in boxplot refers to the 25th percentile data, whereas the top edge of the box refers to the 75th percentile of the data. The bottom and top line refers to the minimum and maximum value respectively. The red line in the middle of the box gives the median value. The mean value of all these parameters are given in Table VI. The total mean computation time is 220.45 seconds.

Almost all the connected PD are identified by the proposed method. The detection does not happen in case of isolated PD. The non-connectivity with the other PDs and region non-neighbourhood to the PD region results in failure to detect the PD. Also some of the retinal grains which are considerably of good contrast is being classified as PD. These are certain factors that badly influences the PD detection. The Figure 11 shows the PDs that are detected and not detected. The regions

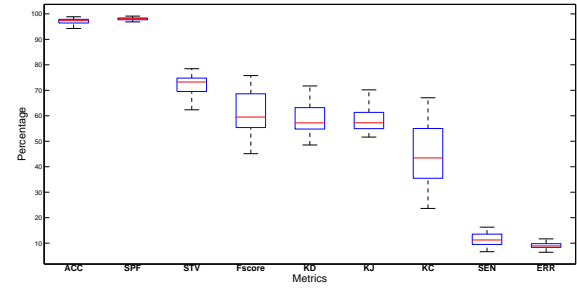


Fig. 9. Accuracy (ACC), specificity (SFP), sensitivity (STV), fscore (FS-CORE), dice coefficient (KD), Jaccard coefficient (KJ), conformity coefficient (KC), sensibility (SEN) and equal error rate (ERR) of 120 images from RIPS dataset with respect to Ground Truth 1

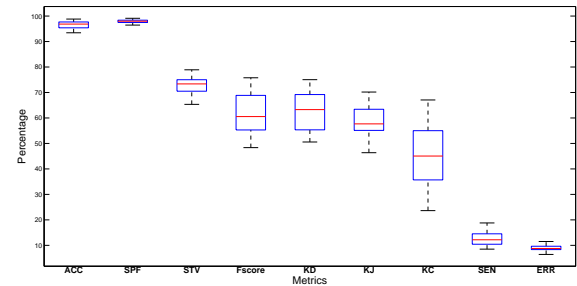


Fig. 10. Accuracy (ACC), specificity (SFP), sensitivity (STV) and fscore (FS-CORE), dice coefficient (KD), Jaccard coefficient (KJ), conformity coefficient (KC), sensibility (SEN) and equal error rate (ERR) of 120 images from RIPS dataset with respect to Ground Truth 2



Fig. 11. Detected PD. The region filled with white color are correctly detected PD, whereas the region filled with red color are the PD which are not detected. The region with blue color are the retinal grains that are wrongly classified as the PD due to high contrast.

filled with white color indicates the detected PD, the region filled with red color indicates the PD that are not detected, and the region filled with blue color indicates the retinal grain regions that are falsely classified as PD.

V. CONCLUSION

This paper discusses in detail about the diagnostic technique of the retinitis pigmentosa with the aid of the imaging

TABLE VI
MEAN VALUE OF METRICS WITH RESPECT TO GROUND TRUTH 1 AND
GROUND TRUTH 2.

PARAMETER	G1	G2
Sensitivity	0.72	0.72
Accuracy	0.96	0.96
Specificity	0.97	0.97
F-score	0.62	0.61
Sensibility	0.12	0.11
Equal error rate	0.09	0.09
Jaccard's coefficient	0.59	0.58
Conformity coefficient	0.45	0.44
Dice coefficient	0.62	0.58
Mean square error	0.038	0.045
Root mean square error	0.0615	0.0865
Peak signal-to-noise ratio	0.84	0.86
Mean absolute error	0.038	0.043
Pearson correlation coefficient	1.8e+005	1.7e+005
Universal quality index	0.91	0.93
Structural content	1.46	1.32
Structural similarity index	0.97	0.96

G1 - performance metrics values with respect to Ground Truth 1

G2 - performance metrics values with respect to Ground Truth 2.

techniques. Even though the RP is incurable, the intensity of the vision degradation can be reduced by some means if it is diagnosed at early stages. There are different methods of imaging including OCT and fundus, the diagnostic made by the fundus seems to be universal and easier. A comprehensive study of the disease RP, its characteristics and its pathological significance is studied in a detailed manner. The blood vessels get attenuated in case of RP patients, and thus the blood vessels of RP patients are extracted using the matched filter and first order derivative of Gaussian. The important characteristics of the pallor of the optic disc is studied by calculating the color indices of the region. This indices is computed for other regions and are also compared. It is also observed that, the Disc Color Indices (DCI1, DCI2, and DCI3) of the RP patients is less than that of the normal persons thus resulting the pale color of the rim. Pigment deposits that characterize the RP is found in the peripheral region of the eye is detected. It is observed that the PDs are darker than other regions of the retinal image. The PDs are classified based on the features (darkness and entropy) and also based on the mahalanobis distance. The MCD estimator is used to define and classify the pigment deposits (PD). The detected PD is compared with the two Ground Truth models which are manually annotated by two experts. Though some of the PD which are isolated and unconnected aren't detected, the performance of the technique is still observed to be in good agreement when various performance metrics are computed. Further some other morphology of the disease is being investigate so as to improve the detection.

REFERENCES

- [1] E. Nakano, M. Hata, A. J. Oishi, K. Miyamoto, A. Uji, M. Fujimoto, M. Miyata, and N. Yoshimura, "Quantitative comparison of disc rim color in optic nerve atrophy of compressive optic neuropathy and glaucomatous optic neuropathy," *Graefes' Archive for Clinical and Experimental Ophthalmology*, vol. 254, pp. 1609–1616, 2016.
- [2] D. C. Hood, M. A. Lazow, K. G. Locke, V. C. Greenstein, and D. G. Birch, "The transition zone between healthy and diseased retina in patients with retinitis pigmentosa," *Investigative Ophthalmology and Visual Science*, vol. 52, no. 1, p. 101, 2011.
- [3] H. Das, A. Saha, and S. Deb, "An expert system to distinguish a defective eye from a normal eye," in *2014 International Conference on Issues and Challenges in Intelligent Computing Techniques (ICICT)*, pp. 155–158, Feb 2014.
- [4] C. Hamel, "Retinitis pigmentosa," *Orphanet Journal of Rare Diseases*, vol. 1, p. 40, Oct 2006.
- [5] Q. Yang, C. A. Reisman, K. Chan, R. Ramachandran, A. Raza, and D. C. Hood, "Automated segmentation of outer retinal layers in macular oct images of patients with retinitis pigmentosa," *Biomed. Opt. Express*, vol. 2, pp. 2493–2503, Sep 2011.
- [6] D. T. Hartong, P. E. L. Berson, and P. T. P. Dryja, "Retinitis pigmentosa," *The Lancet*, vol. 368, no. 9549, pp. 1795–1809, 2006.
- [7] Y. Xu, L. Guan, X. Xiao, J. Zhang, S. Li, H. Jiang, X. Jia, J. Yang, X. Guo, Y. Yin, J. Wang, and Q. Zhang, "Mutation analysis in 129 genes associated with other forms of retinal dystrophy in 157 families with retinitis pigmentosa based on exome sequencing," in *Molecular vision*, 2015.
- [8] P. D. Pozzo, E. Cardaioli, E. Malfatti, G. N. Gallus, A. Malandrini, C. Gaudio, G. Berti, F. Invernizzi, M. Zeviani, and A. Federico, "a novel mutation in the mitochondrial tnapro gene associated with late-onset ataxia, retinitis pigmentosa, deafness, leukoencephalopathy and complex i deficiency," *European journal of human genetics*, vol. 17, pp. 1092–1096, 2009.
- [9] K. Kajiwara, E. L. Berson, and T. P. Dryja, "Digenic retinitis pigmentosa due to mutations at the unlinked peripherin/rds and rom1 loci.," *Science*, vol. 264 5165, pp. 1604–8, 1994.
- [10] L. Li, N. Khan, T. Hurd, A. K. Ghosh, C. Cheng, R. Molday, J. R. Heckenlively, A. Swaroop, and H. Khanna, "Ablation of the x-linked retinitis pigmentosa 2 (rp2) gene in mice results in opsin mislocalization and photoreceptor degeneration," *Investigative Ophthalmology and Visual Science*, vol. 54, no. 7, p. 4503, 2013.
- [11] G. P. Theodossiadis and S. N. Kokolakis, "macular pigment deposits in rhegmatogenous retinal detachment," *British Journal of Ophthalmology*, vol. 63, pp. 498 – 506, Jul 1979.
- [12] M. Frucci, D. Riccio, G. S. di Baja, and L. Serino, "Severe: Segmenting vessels in retina images," *Pattern Recognition Letters*, vol. 82, pp. 162 – 169, 2016. An insight on eye biometrics.
- [13] S. Goswami, S. Goswami, and S. De, "Automatic measurement and analysis of vessel width in retinal fundus image," in *Proceedings of the First International Conference on Intelligent Computing and Communication* (J. K. Mandal, S. C. Satapathy, M. K. Sanyal, and V. Bhateja, eds.), (Singapore), pp. 451–458, Springer Singapore, 2017.
- [14] D. Popescu and L. Ichim, "Intelligent image processing system for detection and segmentation of regions of interest in retinal images," *Symmetry*, vol. 10, no. 3, 2018.
- [15] B. Zhang, L. Zhang, L. Zhang, and F. Karray, "Retinal vessel extraction by matched filter with first-order derivative of gaussian," *Computers in Biology and Medicine*, vol. 40, no. 4, pp. 438 – 445, 2010.
- [16] Q. Yuanzhen, W. Y. Xing, X. Liang, Z. Liwei, Z. Junting, Z. Jianguo, W. Lina, Y. Liu, Y. Anchoo, W. Jian, and J. J. B., "Glaucomalike optic neuropathy in patients with intracranial tumours," *Acta Ophthalmologica*, vol. 89, no. 5, pp. e428–e433, 2011.
- [17] N. Brancati, M. Frucci, D. Gragnaniello, D. Riccio, V. D. Iorio, L. D. Perna, and F. Simonelli, "Learning-based approach to segment pigment signs in fundus images for retinitis pigmentosa analysis," *Neurocomputing*, vol. 308, pp. 159 – 171, 2018.
- [18] N. M. Kumar and D. Samarendra, "Differential entropy in wavelet sub-band for assessment of glaucoma," *International Journal of Imaging Systems and Technology*, vol. 22, no. 3, pp. 161–165.
- [19] K. Udayakumar, P. P. Bharati, S. Verma, and M. K. Nath, "Automatic estimation of vision degradation from color fundus image," *International Journal of Image, Graphics and Signal Processing*, vol. 7, no. 11, pp. 26–34, 2015.